

# Raman spectroscopy of $\text{GaSb}_{1-x}\text{Bi}_x$ alloys with high Bi content

Cite as: Appl. Phys. Lett. **116**, 202103 (2020); <https://doi.org/10.1063/5.0008100>

Submitted: 19 March 2020 . Accepted: 06 May 2020 . Published Online: 20 May 2020

S. Souto, J. Hilska , Y. Galvão Cobato , D. Souza, M. B. Andrade , E. Koivusalo , J. Puustinen, and M. Guina 



View Online



Export Citation



CrossMark

## ARTICLES YOU MAY BE INTERESTED IN

[Local electric field measurement in GaN diodes by exciton Franz-Keldysh photocurrent spectroscopy](#)

Applied Physics Letters **116**, 202102 (2020); <https://doi.org/10.1063/1.5144778>

[Defects in Semiconductors](#)

Journal of Applied Physics **127**, 190401 (2020); <https://doi.org/10.1063/5.0012677>

[Non-metallic electrical transport properties of a metastable  \$\lambda\text{-Ti}\_3\text{O}\_5\$  thin film epitaxially stabilized on a pseudobrookite seed layer](#)

Applied Physics Letters **116**, 201904 (2020); <https://doi.org/10.1063/5.0008888>

Lock-in Amplifiers  
up to 600 MHz



# Raman spectroscopy of $\text{GaSb}_{1-x}\text{Bi}_x$ alloys with high Bi content

Cite as: Appl. Phys. Lett. **116**, 202103 (2020); doi: [10.1063/5.0008100](https://doi.org/10.1063/5.0008100)

Submitted: 19 March 2020 · Accepted: 6 May 2020 ·

Published Online: 20 May 2020



View Online



Export Citation



CrossMark

S. Souto,<sup>1</sup> J. Hilska,<sup>2,a)</sup>  Y. Galvão Cobato,<sup>3</sup>  D. Souza,<sup>3</sup> M. B. Andrade,<sup>4</sup>  E. Koivusalo,<sup>2</sup>  J. Puustinen,<sup>2</sup> and M. Guina<sup>2</sup> 

## AFFILIATIONS

<sup>1</sup>Departamento de Ciências Básicas-Faculdade de Zootecnia e Engenharia de Alimentos, Universidade de São Paulo, CEP 13635-900 Pirassununga, SP, Brazil

<sup>2</sup>Optoelectronics Research Centre, Physics Unit, Tampere University, Korkeakoulunkatu 3, 33720 Tampere, Finland

<sup>3</sup>Departamento de Física, Universidade Federal de São Carlos (UFSCAR), 13560-905 São Carlos, SP, Brazil

<sup>4</sup>São Carlos Institute of Physics, University of São Paulo, PO Box 369, São Carlos, SP 13560-970, Brazil

<sup>a)</sup>Author to whom correspondence should be addressed: [joonas.hilska@tuni.fi](mailto:joonas.hilska@tuni.fi)

## ABSTRACT

We report on the crystal morphology and Raman scattering features of high structural quality  $\text{GaSb}_{1-x}\text{Bi}_x$  alloys grown by molecular beam epitaxy with a high Bi content ( $x$  up to  $\sim 0.10$ ). The Raman spectra were measured at room temperature with different laser excitation wavelengths of 532 nm, 633 nm, and 785 nm. We observed well-defined Bi-induced Raman peaks associated with atomic  $\text{Bi}_n$  clusters and  $\text{GaBi}$  vibrational modes. Remarkably, some Bi-induced Raman modes were strongly enhanced when the laser energy was selected near an optical transition for the 5.8%Bi sample. This effect was attributed to a Raman resonant effect near an excited optical transition of the  $\text{GaSbBi}$  layer and has been used to identify the nature of the observed Raman peaks.

Published under license by AIP Publishing. <https://doi.org/10.1063/5.0008100>

Bismuth-containing III–V alloys have drawn considerable attention in recent years, owing to their potential for near-to-mid-infrared optoelectronics and spintronics applications.<sup>1–7</sup> Importantly, the introduction of Bi into III–V alloys results in a large bandgap reduction and spin–orbit splitting. However, Bi atoms are difficult to incorporate into III–V alloys due to their large size, making the growth of III–V bismides challenging and leading to strict requirements for growth at low temperatures at near-stoichiometric V/III flux ratios.<sup>2–4,8</sup> On the other hand, growth at low temperatures can trigger the formation of various crystalline defects, which have a significant impact on the optical properties. While the majority of early studies have been focused on  $\text{GaAsBi}$  compounds, the incorporation of Bi into  $\text{GaSb}$ -based alloys has recently attracted much attention owing to possible applications in the mid-infrared region. So far, most studies concerning  $\text{GaSbBi}$  have focused on the growth process, structural quality, and optical properties, such as absorption, photoreflectance, and photoluminescence.<sup>2,4,9,10</sup> Yet, there are no reports on Raman spectroscopy for  $\text{GaSbBi}$  layers demonstrating well-defined Bi-related vibrational modes.<sup>1,10</sup> In fact, only a very weak shoulder around  $213\text{--}215\text{ cm}^{-1}$  has been previously reported in the Raman spectra of dilute  $\text{GaSbBi}$  layers (0.4%Bi) associated with a  $\text{GaBi}$  vibrational Raman mode.<sup>10</sup> On the other hand, there are several reports on Raman spectroscopy of

$\text{GaAsBi}$  layers and other Bi-containing materials.<sup>11–19</sup> Despite these investigations, the interpretation of  $\text{GaBi}$ -related Raman peaks is still being unveiled. In fact, as the bulk  $\text{GaBi}$  crystal has not been synthesized, the identification of  $\text{GaBi}$ -related vibrational Raman modes is usually a difficult task. In general, two Bi-related Raman modes are usually observed around  $185$  and  $210\text{ cm}^{-1}$  and are associated with  $\text{TO}(\Gamma)$  and  $\text{LO}(\Gamma)$   $\text{GaBi}$  modes.<sup>15,17</sup> However, this interpretation is not in agreement with several predictions,<sup>18,20,21</sup> which have pointed out a separation of  $\text{TO}(\Gamma)$  and  $\text{LO}(\Gamma)$   $\text{GaBi}$  vibrational modes of less than  $10\text{ cm}^{-1}$ . Moreover, atomic  $\text{Bi}_n$  clusters and disorder-activated modes have been suggested to further complicate the Raman spectra.<sup>18,19,22</sup> Resolving these issues calls for more extensive studies in order to understand the nature of Raman peaks in Bi-containing III–V alloys.

In this Letter, we have investigated the structural and Raman spectroscopic properties of high structural quality  $\text{GaSbBi}$  alloys grown by molecular beam epitaxy (MBE) with a high Bi content. We observed well-defined Bi-induced Raman peaks associated with atomic  $\text{Bi}_n$  clusters and  $\text{GaBi}$  vibrational modes. Remarkably, we have shown that by selecting the laser energy close to an excited transition of the  $\text{GaSbBi}$  semiconductor material, several Bi-induced Raman vibrational modes become clearly enhanced. We explain this effect via a resonant

Raman effect near the E1 interband transition. In particular, we have used the resonant Raman effect and polarized Raman spectroscopy to identify the nature of the observed Raman peaks.

Three GaSbBi samples (B1, B2, and B3) and a reference GaSb sample (R) were grown by MBE on n-GaSb(100) substrates. All samples were grown at a temperature of 350 °C following the growth procedure described in our previous work,<sup>4</sup> with the exception that the substrates were rotated during growth to produce uniform compositions across the wafers. The GaSbBi structures were grown under near-stoichiometric Sb/Ga flux ratios and different Bi/Ga beam equivalent pressure ratios of 0.08 (B1), 0.11 (B2), and 0.14 (B3). The growth temperatures were measured using a thermocouple and are consistent with our previous work.<sup>4</sup>

High-resolution x-ray diffraction (HR-XRD)  $\omega$ -2θ scans from the (400) reflection were used to investigate the structural quality. The Bi contents were determined by fitting simulations based on the dynamical theory of x-ray diffraction to the HR-XRD data. Fully pseudomorphic layers and Vegard's law with a lattice constant of 6.27 Å<sup>9</sup> for the GaBi binary were assumed in the simulations. The fully pseudomorphic growth was confirmed by reciprocal space mapping (RSM). The surfaces were characterized by atomic force microscopy (AFM), to exclude effects from surface imperfections.

Polarization-dependent Raman spectra were measured at room temperature using a Renishaw inVia Qontor Raman microscope with a 785 nm laser. The measurements were performed in quasi-backscattering Porto geometry  $\bar{Z}(XX)Z$  and  $\bar{Z}(XY)Z$  with the basis  $X = [0\bar{1}1]$ ,  $Y = [01\bar{1}]$ , and  $Z = [100]$ . For non-polarized micro-Raman measurements, we used different laser wavelengths, i.e., 532 nm, 633 nm, and 785 nm, and a Horiba LabRAM HR Evolution system with a 1800 g/mm grating and a 50× objective. In all Raman experiments, the spectral resolution was  $\sim 1 \text{ cm}^{-1}$  and the laser power densities were below 1 W/cm<sup>2</sup> to avoid sample heating.

Figure 1 compiles the HR-XRD  $\omega$ -2θ data (solid lines) overlaid by their respective simulations (dotted lines) for all the samples

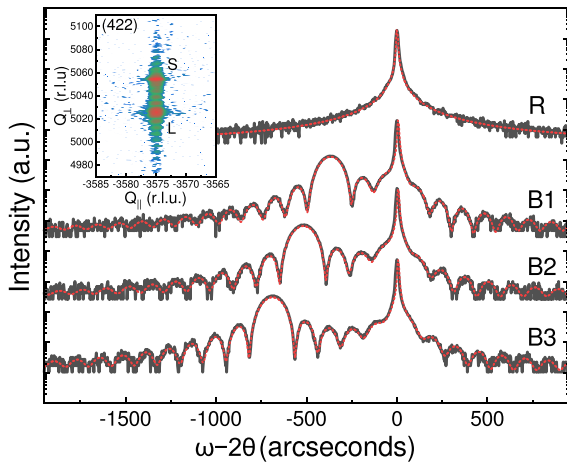


FIG. 1. HR-XRD measurements (solid gray) and simulations (dotted red) from all the reported samples. The  $\omega$ -2θ axis is centered to the GaSb(400) reflection, and the samples are labeled near the right-hand side axis. The inset shows the RSM from sample B3 corresponding to the (422) diffraction, with the substrate and epilayer peaks designated with S and L.

reported. The reference sample R exhibits a single intense and narrow peak corresponding to the GaSb(400) reflection, indicating that the grown epilayer is perfectly lattice-matched to the substrate. In fact, the FWHM of the diffraction peak is only  $\sim 11.3$  arcseconds and the data can be fitted with high accuracy by assuming an infinitely thick GaSb layer in the model. In contrast, all the Bi-containing samples (B1–B3) show clear intense secondary peaks corresponding to the GaSbBi epilayers, which are offset from the substrate peak by varying degrees based on the amount of compressive strain, which is proportional to the Bi content. In addition, the GaSbBi peaks are surrounded by clear Pendellösung oscillations, which indicates high interface quality and homogeneous Bi content. Based on the simulations, which follow the experimental data closely, the Bi contents are 5.8% (B1), 8.0% (B2), and 10.6% (B3). To confirm that no relaxation has occurred, a RSM from sample B3 was measured and is shown in the top-left inset of Fig. 1. In the RSM, the substrate and epilayer peaks are aligned on the in-plane reciprocal space axis, indicating that no relaxation of the epilayer has occurred. Since samples B1 and B2 have the same thickness and lower strain, none of the samples are expected to be relaxed. To further exclude effects from structural imperfections, the surface quality was characterized by AFM. All the samples exhibited droplet-free smooth surfaces, with RMS roughnesses below 0.5 nm. A more detailed AFM analysis can be found in the [supplementary material](#) (cf. Fig. S1).

Figure 2 shows typical room temperature Raman spectra of samples with different Bi contents (B1–B3) and of the reference GaSb sample (R) measured with 785 nm excitation in the  $\bar{Z}(XX)Z$  configuration. The Raman spectra in the  $\bar{Z}(XY)Z$  configuration are shown in Fig. S2 (see the [supplementary material](#)). Raman peaks around 114 cm<sup>-1</sup>, 162 cm<sup>-1</sup>, 235.5 cm<sup>-1</sup>, and 269 cm<sup>-1</sup> are observed for all samples, which is consistent with peaks observed in the literature for the bulk GaSb crystal.

These peaks are usually associated with the crystalline GaSb Zinc blende structure, point group  $T_d$  43m, which shows second order: 2TA(X and  $\Sigma$ ) ( $111 \pm 3 \text{ cm}^{-1}$  and  $117 \pm 3 \text{ cm}^{-1}$ ) and 2TA(W and Q) ( $160 \pm 5 \text{ cm}^{-1}$ ), first order: TO( $\Gamma$ ) ( $227.1 \pm 1.0 \text{ cm}^{-1}$ ) and LO( $\Gamma$ )

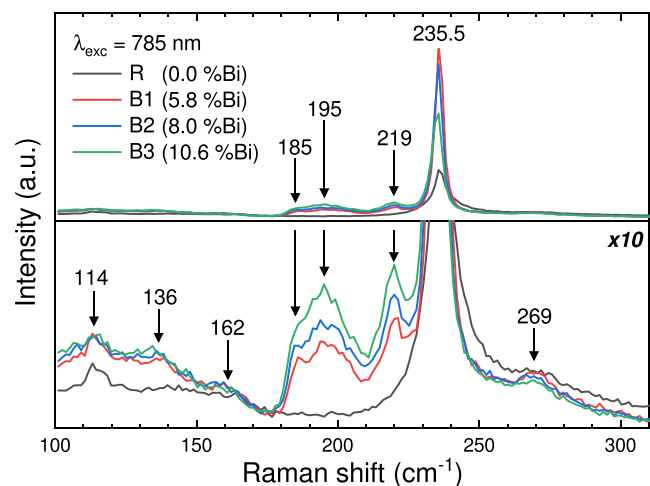


FIG. 2. Raman spectra for different Bi contents using 785 nm laser excitation measured in the  $\bar{Z}(XX)Z$  configuration.

( $237.1 \pm 1.0 \text{ cm}^{-1}$ ), and second order:  $\text{TO}(X) + \text{TA}(X)$  ( $272 \pm 3 \text{ cm}^{-1}$ ) vibrational modes.<sup>23,24</sup> Particularly, the most intense Raman peak around  $235.5 \text{ cm}^{-1}$  is associated with the  $\text{LO}(\Gamma)$  GaSb mode. We point out that this mode shows a clear red shift with increasing %Bi (Fig. S3), indicating an increase in compressive strain, in agreement with the HR-XRD results. Moreover, the linewidth of the  $\text{LO}(\Gamma)$  GaSb mode increases as the Bi content is increased. These effects are associated with an increase in disorder with the increasing Bi content.

In comparison to the Bi-free sample (R), the GaSbBi samples (B1-B3) show several additional Raman peaks around  $136 \text{ cm}^{-1}$ ,  $185 \text{ cm}^{-1}$ ,  $195 \text{ cm}^{-1}$ , and  $219 \text{ cm}^{-1}$ . Particularly, the peak at  $219 \text{ cm}^{-1}$  has a higher value than the peak usually associated with the  $\text{LO}(\Gamma)$  GaBi vibrational mode around  $210 \text{ cm}^{-1}$  in GaAsBi layers.<sup>15,17</sup> However, the polarized Raman results (Fig. S2) show that this peak has different polarization behavior from the  $\text{LO}(\Gamma)$  GaSb vibrational mode, which makes this interpretation partially inconsistent. Moreover, this peak is at a much higher frequency than the theoretical value predicted for the  $\text{LO}(\Gamma)$  GaBi Raman mode.<sup>20,21</sup> Correspondingly, the Raman peak observed at  $185 \text{ cm}^{-1}$ , which has the same polarization as the  $\text{LO}(\Gamma)$  GaSb vibrational mode (Fig. S2), was previously observed in several studies on GaAsBi<sup>15,18,19,25,26</sup> and was associated with the  $\text{TO}(\Gamma)$  GaBi vibrational mode, which is also inconsistent with our polarized Raman results. Particularly, this mode attribution implies a separation of  $34 \text{ cm}^{-1}$  between the  $\text{LO}(\Gamma)$  and  $\text{TO}(\Gamma)$  GaBi modes, which is much larger than the predicted separation of less than  $10 \text{ cm}^{-1}$ .<sup>18,20,21</sup> Therefore, we attribute the Raman peak observed around  $185 \text{ cm}^{-1}$  to be a convoluted  $\text{LO}(\Gamma) + \text{TO}(\Gamma)$  GaBi vibrational mode. This attribution is more consistent with the previous predictions<sup>18,20,21</sup> for the Raman peak positions as well as for the frequency separation between the  $\text{TO}(\Gamma)$  and  $\text{LO}(\Gamma)$  GaBi modes. Moreover, instead of the  $\text{LO}(\Gamma)$  GaBi mode, the Raman peak around  $219 \text{ cm}^{-1}$  could be associated with GaSb Raman vibrational modes due to other zone boundaries, such as  $\text{TO}(X)$  and/or  $\text{TO}(L)$ ,<sup>24</sup> which are forbidden by the typical momentum conservation rules for first-order Raman scattering in GaSb. Observation of the forbidden modes could be explained by Bi-induced disorder in the lattice, leading to the relaxation of Raman selection rules, as proposed in several previous works.<sup>24,27</sup> In the resonant condition (Fig. 3), the appearance of the GaSb-like  $\text{TO}(X)$  or  $L$  phonon mode in the GaSbBi Raman spectra could be associated with Bi-induced mixing of the GaSb valence band. A similar effect was observed for the GaAsN semiconductor and attributed to the N-induced mixing of GaAs conduction bands.<sup>28,29</sup> However, a possible contribution of the longitudinal-optical-plasmon-coupled mode should also be considered. Therefore, further studies would be necessary for a complete understanding of the nature of this Raman peak.

At the other end of the spectrum, the Raman peak around  $136 \text{ cm}^{-1}$  has too low frequency to be associated with any LO or TO GaBi modes. In fact, this Raman peak is in the acoustic regime and is usually associated with disorder activated longitudinal acoustic (DALA) modes induced by Bi.<sup>27</sup> On the other hand, it could also be attributed to vibration modes of atomic  $\text{Bi}_n$  clusters, consistent with the fact that Bi atoms are not easily incorporated into the crystalline structure. The Bi incorporation into GaSbBi films has been generally reported to be over 97% substitutional in the group-V sublattice,<sup>9,30</sup> translating to a low concentration of pure atomic  $\text{Bi}_n$  clusters, where

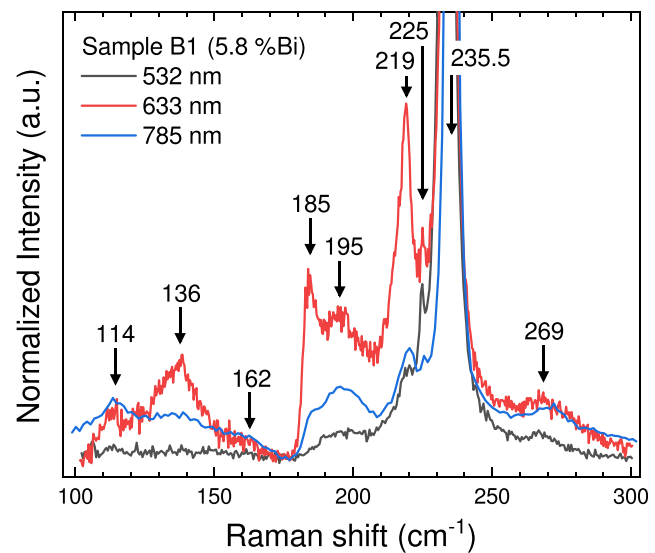


FIG. 3. Non-polarized Raman spectra of sample B1 with different excitation wavelengths. The intensities have been normalized to the  $\text{LO}(\Gamma)$  GaSb mode.

some Bi atoms occupy other than substitutional sites. However, Punkkinen *et al.*<sup>31</sup> reported that Bi clustering in GaAsBi is driven by the existence of Ga vacancies in the lattice. Moreover, Ga vacancies in GaSbBi have been recently shown to contribute to large hole densities in GaSbBi.<sup>32</sup> Thus, there is a clear rationale for why such clusters would exist in these high Bi content GaSbBi materials. Therefore, these results lead us to tentatively attribute this peak to a combination of DALA and/or atomic  $\text{Bi}_4$  cluster modes, which have shown Raman peaks near the observed peak around  $136 \text{ cm}^{-1}$ .<sup>22</sup> Finally, the peak at  $195 \text{ cm}^{-1}$  is not observed in the large majority of literature studies related to Bi-containing materials. However, a study on Bi-doped glasses<sup>33</sup> and a theoretical prediction<sup>22</sup> found a vibrational mode around  $195 \text{ cm}^{-1}$  related to the  $\text{Bi}_2$  dimer. Therefore, we suggest this  $\text{Bi}_2$  mode as the origin of the observed peak at  $195 \text{ cm}^{-1}$ . We do note that the higher Bi content as compared to previous studies of other III-V bismides could favor the formation of  $\text{Bi}_2$  dimers and, thus, explain its absence in previous studies.

We have also measured Raman spectra using different excitation wavelengths of 532 and 633 nm. Figure 3 shows the Raman spectra of sample B1 (5.8%Bi) for all excitation wavelengths. Again, the most intense Raman peak around  $235.5 \text{ cm}^{-1}$  is the  $\text{LO}(\Gamma)$  GaSb mode and the small peak at  $225 \text{ cm}^{-1}$  is associated with the  $\text{TO}(\Gamma)$  GaSb mode.<sup>23</sup> The observation of the  $\text{TO}(\Gamma)$  GaSb mode evidences the presence of disorder induced by Bi atoms as the  $\text{TO}(\Gamma)$  peak is forbidden by the selection rules. The spectrum measured using 532 nm excitation shows the same features as those observed for the 785 nm excitation, but with less distinct peaks and lower signal-to-noise ratios in the region of Bi-induced modes. Conversely, the Raman spectrum for 633 nm excitation shows particularly distinct peaks related to the Bi-induced modes.

Remarkably, the Raman peaks at 219, 185, and  $136 \text{ cm}^{-1}$  are strongly enhanced under 633 nm excitation. This can be explained by the resonant Raman effect as the laser excitation at 1.96 eV (633 nm) is near an excited optical transition of the GaSbBi material. Some

**TABLE I.** Summary of the observed Raman peaks and their properties.

Wavenumber (cm <sup>-1</sup> )	Assignment	Selection rule <sup>a</sup>		Order	Bi induced
114	2TA(X + $\Sigma$ )	Allowed	Forbidden		x
136	DALA	Forbidden	Forbidden	x	x
162	2TA(W + Q)	Allowed	Forbidden		x
185	LO( $\Gamma$ ) + TO( $\Gamma$ ) GaBi	Allowed	Forbidden	x	x
195	Bi <sub>2</sub> dimer	Allowed	Forbidden	x	x
219	TO(X)/TO(L) GaSb	Forbidden	Forbidden	x	x
225	TO( $\Gamma$ ) GaSb	Forbidden	Forbidden	x	
235.5	LO( $\Gamma$ ) GaSb	Allowed	Forbidden	x	
269	TO(X) + TA(X) GaSb	Allowed	Forbidden		x

<sup>a</sup>For a perfect bulk crystal. Note that many forbidden modes are observed in the Raman spectra by Bi-induced disorder and relaxation of the selection rules.

theoretical studies on the band structure of GaSbBi<sup>34–36</sup> have used the popular valence band anti-crossing model (VBAC) and have shown a transition between the LH/HH<sup>+</sup> valence sub-band and the conduction band, which would be around the 633 nm laser excitation energy for 5.8%Bi. However, Polak *et al.*<sup>37</sup> showed that the VBAC model is less valid for GaSbBi alloys, owing to the weaker chemical dissimilarity between Sb and Bi, than, for example, As or P and Bi. In fact, theoretical calculations based on the density functional theory show that an interband transition on the  $\Lambda$ -line has an energy gap near the 633 nm laser energy (i.e., the E1 transition), particularly for a Bi content close to 5.8%Bi,<sup>38,39</sup> which is more likely the resonant transition.

We find the resonant Raman results to be fully consistent with the above discussion on the nature of observed peaks. Namely, the 136 cm<sup>-1</sup> and 185 cm<sup>-1</sup> Raman peaks are extremely sensitive to the resonant condition, have the same polarization as the GaSb LO mode, and are also observed in GaAsBi layers. Previously, we tentatively ascribed the 136 cm<sup>-1</sup> mode to DALA and/or Bi<sub>4</sub> clusters based on earlier reports.<sup>22,27</sup> Considering that this mode is sensitive to the resonant condition, we can now rule out the contribution of atomic Bi<sub>4</sub> clusters, as they are not expected to have a resonant optical transition at the wavelength of 633 nm. Conversely, the modes at 185 cm<sup>-1</sup>, TO( $\Gamma$ ) and LO( $\Gamma$ ) of GaBi in the GaSbBi alloy, are resonant due to the E1 gap as expected. Interestingly, the 219 cm<sup>-1</sup> peak is also sensitive to the resonant condition, but has different polarization from the LO( $\Gamma$ ) GaSb mode. Therefore, we suggest that the 219 cm<sup>-1</sup> Raman peak is associated with other zone boundaries of GaSb Raman vibrational modes, such as TO(X) and TO(L),<sup>27</sup> which could be allowed by increased disorder due to Bi incorporation. Again, this interpretation is consistent with the polarized Raman spectra. Furthermore, it is expected that this GaSb vibrational mode could be resonant to the E1 gap absorption of the GaSbBi crystal. Finally, the 195 cm<sup>-1</sup> peak is not sensitive to the resonant condition. In fact, our results indicate that the 195 cm<sup>-1</sup> peak has a different nature and could indeed be associated with the vibration of the dimer Bi<sub>2</sub>, which is not coupled to vibrational modes related to GaSb.<sup>22,33</sup> As a summary of the above discussion, all the observed Raman peaks are compiled in Table I.

In conclusion, we have observed several distinct peaks in the Raman spectra (non-polarized and polarized) of GaSbBi layers, which are not visible in GaSb grown under similar conditions. We have

observed a resonant Raman effect in a GaSbBi layer with 5.8%Bi using 633 nm excitation, which enhanced some of the Bi-induced Raman peaks. The resonant Raman effect and polarized Raman results were used to investigate and characterize the nature of the observed Raman peaks. Particularly, the Raman peak observed at 185 cm<sup>-1</sup> was associated with a convoluted LO( $\Gamma$ ) + TO( $\Gamma$ ) GaBi mode. The Raman peaks observed at 136 cm<sup>-1</sup>, 195 cm<sup>-1</sup>, and 219 cm<sup>-1</sup> were associated with DALA, atomic Bi<sub>2</sub> cluster, and TO(X)/TO(L) GaSb phonon modes, respectively.

See the [supplementary material](#) for additional AFM and Raman measurements supporting the conclusions made in this study.

This work was supported by the Brazilian agencies “Fundação de Amparo a Pesquisa do Estado de São Paulo” (FAPESP) (Grant Nos. 16/10668-7 and 14/50513-7) and “Conselho Nacional de Desenvolvimento Científico e Tecnológico” (CNPq), the ERC AdG Project AMETIST (Grant No. ERC-2015-AdG 695116), and is also part of Academy of Finland Flagship Programme PREIN No. 320168. The authors acknowledge the experimental support received from the Microscopy Center facilities at Tampere University.

## DATA AVAILABILITY

The data that support the findings of this study are available from the corresponding author upon reasonable request.

## REFERENCES

- 1 S. Wang and P. Lu, *Bismuth-Containing Alloys and Nanostructures* (Springer, 2019).
- 2 O. Delorme, L. Cerutti, E. Tournié, and J.-B. Rodriguez, “Molecular beam epitaxy and characterization of high Bi content GaSbBi alloys,” *J. Cryst. Growth* **477**, 144–148 (2017).
- 3 X. Lu, D. A. Beaton, R. B. Lewis, T. Tiedje, and M. B. Whitwick, “Effect of molecular beam epitaxy growth conditions on the Bi content of GaAsBi,” *Appl. Phys. Lett.* **92**, 192110 (2008).
- 4 J. Hilska, E. Koivusalo, J. Puustinen, S. Suomalainen, and M. Guina, “Epitaxial phases of high Bi content GaSbBi alloys,” *J. Cryst. Growth* **516**, 67–71 (2019).
- 5 A. R. H. Carvalho, V. Orsi Gordo, H. V. A. Galeti, Y. Galvão Gobato, M. P. F. de Godoy, R. Kudrawiec, O. M. Lemine, and M. Henini, “Magneto-optical properties of GaBiAs layers,” *J. Phys. D: Appl. Phys.* **47**, 075103 (2014).

<sup>6</sup>O. Delorme, L. Cerutti, E. Luna, G. Narcy, A. Trampert, E. Tournié, and J.-B. Rodriguez, “GaSbBi/GaSb quantum well laser diodes,” *Appl. Phys. Lett.* **110**, 222106 (2017).

<sup>7</sup>M. Gladysiewicz, R. Kudrawiec, and M. S. Wartak, “Electronic band structure and material gain of III-V-Bi quantum wells grown on GaSb substrate and dedicated for mid-infrared spectral range,” *J. Appl. Phys.* **119**, 075701 (2016).

<sup>8</sup>J. Puustinen, J. Hilska, and M. Guina, “Analysis of GaAsBi growth regimes in high resolution with respect to As/Ga ratio using stationary MBE growth,” *J. Cryst. Growth* **511**, 33–41 (2019).

<sup>9</sup>M. K. Rajpalke, W. M. Linhart, M. Birkett, K. M. Yu, J. Alaria, J. Kopaczek, R. Kudrawiec, T. S. Jones, M. J. Ashwin, and T. D. Veal, “High Bi content GaSbBi alloys,” *J. Appl. Phys.* **116**, 043511 (2014).

<sup>10</sup>S. Das, T. Das, S. Dhar, M. de la Mare, and A. Krier, “Near infrared photoluminescence observed in dilute GaSbBi alloys grown by,” *Infrared Phys. Technol.* **55**, 156–160 (2012).

<sup>11</sup>R. S. Joshya, V. Rajaji, C. Narayana, A. Mascarenhas, and R. Kini, “Anharmonicity in light scattering by optical phonons in GaAs<sub>1-x</sub>Bi<sub>x</sub>,” *J. Appl. Phys.* **119**, 205706 (2016).

<sup>12</sup>F. Sarcan, Ö. Dönmez, K. Kara, A. Erol, E. Akalin, M. Ç. Arıkan, H. Makhlofui, A. Arnoult, and C. Fontaine, “Bismuth-induced effects on optical, lattice vibrational, and structural properties of bulk GaAsBi alloys,” *Nanoscale Res. Lett.* **9**, 119 (2014).

<sup>13</sup>T. M. Christian, B. Fluegel, D. A. Beaton, A. Kirstin, and A. Mascarenhas, “Bismuth-induced Raman modes in GaP<sub>1-x</sub>Bi<sub>x</sub>,” *Jpn. J. Appl. Phys., Part 1* **55**, 108002 (2016).

<sup>14</sup>S. Yoon, M. J. Seong, B. Fluegel, and A. Mascarenhas, “Photogenerated plasmons in GaAs<sub>1-x</sub>Bi<sub>x</sub>,” *Appl. Phys. Lett.* **91**, 082101 (2007).

<sup>15</sup>J. A. Steele, R. A. Lewis, M. Henini, O. M. Lemine, D. Fan, Y. Mazur, V. G. Dorogan, P. C. Grant, S.-Q. Yu, and G. J. Salamo, “Raman scattering reveals strong LO-phonon-hole-plasmon coupling in nominally undoped GaAsBi: Optical determination of carrier concentration,” *Opt. Express* **22**, 11680 (2014).

<sup>16</sup>W. Pan, J. A. Steele, P. Wang, K. Wang, Y. Song, L. Yue, X. Wu, H. Xu, Z. Zhang, S. Xu, P. Lu, L. Wu, Q. Gong, and S. Wang, “Raman scattering studies of dilute InP<sub>1-x</sub>Bi<sub>x</sub> alloys reveal unusually strong oscillator strength for Bi induced modes,” *Semicond. Sci. Technol.* **30**, 094003 (2015).

<sup>17</sup>J. A. Steele, R. A. Lewis, M. Henini, O. M. Lemine, and A. Alkaoud, “Raman scattering studies of strain effects in (100) and (311)B GaAs<sub>1-x</sub>Bi<sub>x</sub> epitaxial layers,” *J. Appl. Phys.* **114**, 193516 (2013).

<sup>18</sup>P. Verma, K. Oe, M. Yamada, H. Harima, M. Herms, and G. Irmer, “Raman studies on GaAs<sub>1-x</sub>Bi<sub>x</sub> and InAs<sub>1-x</sub>Bi<sub>x</sub>,” *J. Appl. Phys.* **89**, 1657–1663 (2001).

<sup>19</sup>M. Seong, S. Francoeur, S. Yoon, A. Mascarenhas, S. Tixier, M. Adamczyk, and T. Tiedje, “Bi-induced vibrational modes in GaAsBi,” *Superlattices Microstruct.* **37**, 394 (2005).

<sup>20</sup>R. Pilevar Shahri and A. Akhtar, “First principles study and comparison of vibrational and thermodynamic properties of XBi (X=In, Ga, B, Al),” *Chin. Phys. B* **26**, 093107 (2017).

<sup>21</sup>A. Belabbes, A. A. Zaoui, and M. Ferhat, “Lattice dynamics study of bismuth III-V compounds,” *J. Phys.: Condens. Matter* **20**, 415221 (2008).

<sup>22</sup>D. Liang, W. Shen, C. Zhangy, P. Lu, and S. Wang, “Structural, electronic, vibrational and optical properties of Bi<sub>n</sub> clusters,” *Mod. Phys. Lett. B* **31**, 1750260 (2017).

<sup>23</sup>P. B. Klein and R. K. Chang, “Comparison of second-order Raman scattering measurements with a phonon density-of-states calculation in GaSb,” *Phys. Rev. B* **14**, 2498 (1976).

<sup>24</sup>T. Sekine, K. Uchinokura, and E. Matsuura, “Two-phonon Raman scattering in GaSb,” *Solid State Commun.* **18**, 1337 (1976).

<sup>25</sup>J. Li, K. Forghani, Y. Guan, W. Jiao, W. Kong, K. Collar, T.-H. Kim, T. F. Kuech, and A. S. Brown, “GaAs<sub>1-y</sub>Bi<sub>y</sub> Raman signatures: Illuminating relationships between the electrical and optical properties of GaAs<sub>1-y</sub>Bi<sub>y</sub> and Bi incorporation,” *AIP Adv.* **5**, 067103 (2015).

<sup>26</sup>P. Wang, W. Pan, X. Wu, C. Cao, S. Wang, and Q. Gong, “Heteroepitaxy growth of GaAsBi on Ge(100) substrate by gas source molecular beam epitaxy,” *Appl. Phys. Express* **9**, 045502 (2016).

<sup>27</sup>R. Cusco, L. Artus, and K. Benzt, “First- and second-order Raman scattering of the Al<sub>x</sub>Ga<sub>1-x</sub>Sb alloy for x = 0.14,” *J. Phys.: Condens. Matter* **7**, 7069 (1995).

<sup>28</sup>H. M. Cheong, Y. Zhang, A. Mascarenhas, and J. F. Geisz, “Nitrogen-induced levels in GaAs<sub>(1-x)</sub>N<sub>(x)</sub> studied with resonant Raman scattering,” *Phys. Rev. B* **61**, 13687 (2000).

<sup>29</sup>M. J. Seong, A. Mascarenhas, and J. F. Geisz, “Γ–L–X mixed symmetry of nitrogen-induced states in GaAs<sub>(1-x)</sub>N<sub>(x)</sub> probed by resonant Raman scattering,” *Appl. Phys. Lett.* **79**, 1297 (2001).

<sup>30</sup>M. K. Rajpalke, W. M. Linhart, K. M. Yu, T. S. Jones, M. J. Ashwin, and T. D. Veal, “Bi flux-dependent MBE growth of GaSbBi alloys,” *J. Cryst. Growth* **425**, 241–244 (2015).

<sup>31</sup>M. P. J. Punkkinen, P. Laukkonen, M. Kuzmin, H. Leväniemi, J. Lång, M. Tuominen, M. Yasir, J. Dahl, S. Lu, and E. K. Delczeg-Czirjak, “Does Bi form clusters in GaAs<sub>1-x</sub>Bi<sub>x</sub> alloys?,” *Semicond. Sci. Technol.* **29**, 115007 (2014).

<sup>32</sup>N. Segercrantz, J. Slotte, I. Makkonen, F. Tuomisto, I. C. Sandall, M. J. Ashwin, and T. D. Veal, “Hole density and acceptor-type defects in MBE-grown GaSb<sub>1-x</sub>Bi<sub>x</sub>,” *J. Phys. D: Appl. Phys.* **50**, 295102 (2017).

<sup>33</sup>V. O. Sokolov, V. Plotnichenko, V. Koltashev, and E. M. Diano, “Centres of broadband near-IR luminescence in bismuth-doped glasses,” *J. Phys. D: Appl. Phys.* **42**, 095410 (2009).

<sup>34</sup>I. Mal, D. Samajdar, and T. D. Das, “Calculation of band structure and optical gain of type-II GaSbBi/GaAs quantum wells using 14-band k-p Hamiltonian,” *Superlattices Microstruct.* **109**, 442 (2017).

<sup>35</sup>S. Das, M. K. Bhowal, and S. Dhar, “Calculation of the band structure, carrier effective mass, and the optical absorption properties of GaSbBi alloys,” *J. Appl. Phys.* **125**, 075705 (2019).

<sup>36</sup>D. P. Samajdar, T. D. Das, and S. Dhar, “Valence band anticrossing model for GaSb<sub>1-x</sub>Bi<sub>x</sub> and GaP<sub>1-x</sub>Bi<sub>x</sub> using k-p method,” *Mater. Sci. Semicond. Process.* **40**, 539 (2015).

<sup>37</sup>M. Polak, P. Scharoch, and R. Kudrawiec, “First-principles calculations of bismuth induced changes in the band structure of dilute Ga-V-Bi and In-V-Bi alloys: Chemical trends versus experimental data,” *Semicond. Sci. Technol.* **30**, 094001 (2015).

<sup>38</sup>R. Kudrawiec, J. Kopaczek, O. Delorme, M. P. Polak, M. Gladysiewicz, E. Luna, L. Cerutti, E. Tournié, and J. B. Rodriguez, “Type I GaSb<sub>1-x</sub>Bi<sub>x</sub>/GaSb quantum wells dedicated for mid infrared laser applications: Photoreflectance studies of bandgap alignment,” *J. Appl. Phys.* **125**, 205706 (2019).

<sup>39</sup>M. P. Polak, P. Scharoch, R. Kudrawiec, J. Kopaczek, M. J. Winiarski, W. M. Linhart, M. K. Rajpalke, K. M. Yu, T. S. Jones, M. J. Ashwin, and T. D. Veal, “Theoretical and experimental studies of electronic band structure for GaSb<sub>1-x</sub>Bi<sub>x</sub> in the dilute Bi regime,” *J. Phys. D: Appl. Phys.* **47**, 355107 (2014).